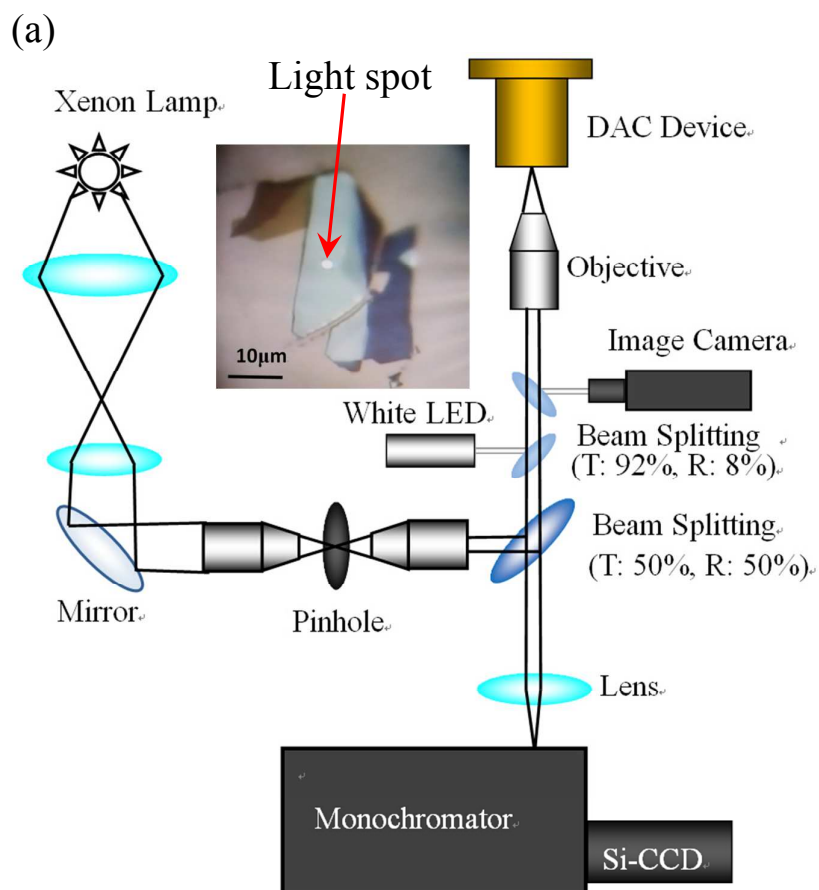# Supporting Information

Probing Spin-Orbit Coupling and Interlayer Coupling in Atomically Thin Molybdenum Disulfide Using Hydrostatic Pressure

Xiuming Dou, Kun Ding, Desheng Jiang, Xiaofeng Fan, and Baoquan Sun
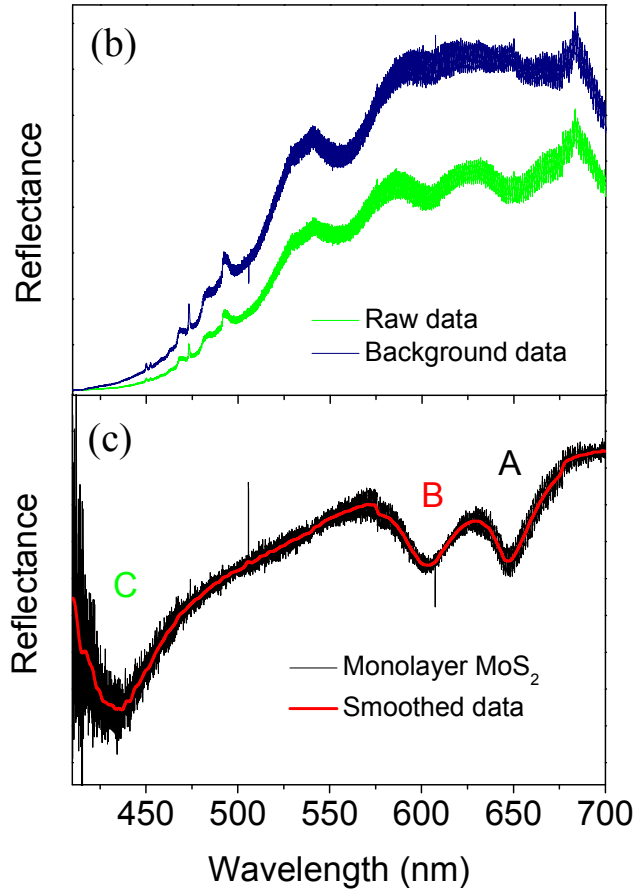
Experimental setup

(a)

Figure S1. (a) Schematic diagram of the experimental setup. The light spot with a size of approximately 2 μm is shown in the inset. (b) Raw data and background data measured at positions of the monolayer MoS_2 sample and the SiO_2/Si substrate, respectively, at pressure of 0.58GPa. (c) The reflectance spectrum of the monolayer MoS_2 at pressure of 0.58 GPa.

The reflectance spectra of atomically thin MoS_2 are carried out using the experimental setup shown in Figure S1. The white light emitting from the Xenon lamp is first spatial shaped to become parallel beam by a pair of 50X objective (NA: 0.4) and a pinhole (diameter: 5μm), and is reflected by a 50:50 beam splitting, then is focused to sample by a long-working-distance objective. The light spot with size of approximately 2 μm shown in the inset is focused by a 100X objective (NA: 0.9). For pressure measurements, the sample is put into the pressure chamber, and a 50X objective (NA:0.35) is used. The reflected light by the sample is collected by the same objective, passes through the 50:50 beam splitting, and then is focused by a lens (focal length: 100 mm) to a monochromator (focal length: 550 mm) equipped with a silicon charge-coupled device (CCD). In order to eliminate the influence of the spectral response of the setup and the absorption of the SiO_2/Si substrate (adding the diamond anvils and liquid argon if the sample is put into the DAC device), the reflectance

spectrum (Figure S1c) of the monolayer MoS_2 is obtained by dividing the reflected raw data of the sample by the background data measured at the position of SiO_2/Si substrate (Figure S1b). For viewing the position of the few-layer MoS_2 sample and the ruby chip, a white LED source, two thin beam splitters (T: 92%, R:8%), and a digital CMOS image camera are used.

Computational method

The present calculations are performed based density functional theory (DFT) using accurate frozen-core full-potential projector augmented-wave (PAW) pseudopotentials, as implemented in the VASP code. The generalized gradient approximation (GGA) with the parametrization of Perdew-Burke-Ernzerhof (PBE) and added van der Waals corrections is used. The k-space integrals and the plane-wave basis sets are chosen to ensure that the total energy is converged at the 1 meV/atom level. A kinetic energy cutoff of 500 eV is found to be sufficient for the plane wave expansion. The effect of dispersion interaction is included by the empirical correction scheme of Grimme (DFT+D/PBE). This approach has been successful in describing graphene-based structures. For the different layered MoS_2, the supercells are constructed with a vacuum space of 20 Å along z direction. The Brillouin zones are sampled with the Γ-centered k-point grid of 18×18×1. With the state-of-the-art method of adding the stress to stress tensor in VASP code, the structure of bulk MoS_2 can be optimized under a specified hydrostatic pressure. With these structural parameters from bulk MoS_2, the single-, double- and triple-layer MoS_2 structures under different pressures were constructed. The band structures are calculated with the consideration of spin-orbit coupling.
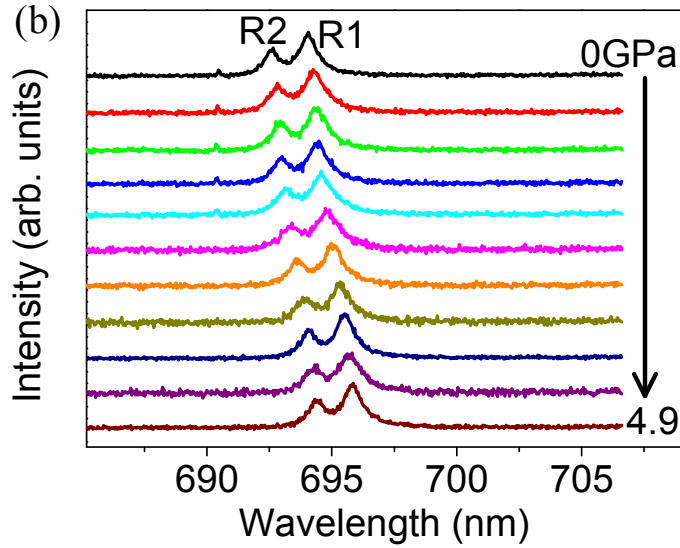
Diamond anvil cell (DAC) device

Figure S2. (a) The photographs of the DAC device. (b) PL spectra of the ruby as the pressure increasing from 0 to 4.9 GPa.

Figure S2a shows the photographs of the DAC device. It is composed of outer cylinder, inner piston, driving screws, gasket and diamond anvils. Both outer cylinder and inner piston are made of beryllium copper and used to transmit the pressure to the DAC. The center part of the DAC device is composed of a pair of diamond anvils with culet diameter of about 700 μm and a 500-μm-thick gasket (T301 stainless steel) as shown in Figure 1b in the main text. The gasket is first incused, and then a hole is drilled in the center of the incused position. The pressure chamber of the DAC with a diameter of ~ 350 μm and a height of ~ 300 μm is made, as shown in Figure 1c in the main text. The SiO_2/Si substrate is approximately 50 nm SiO_2 on Si substrate by thermal oxidation. Then, the SiO_2/Si substrate is mechanically thinned to approximately 100 μm. The few-layer MoS_2 is micro-mechanically exfoliated and transferred to the thinned substrate, then, the substrate with few-layer MoS_2 is cleaved to a size of approximately 300×300 μm^2 by using a micro-positioned pin, finally, the cleaved sample is put into the pressure chamber. Liquid Argon is used as the pressure transmitting medium (PTM) in the DAC which shows a good hydrostatic pressure behavior at room temperature[1]. Hydrostatic pressure generated inside the pressure chamber is monitored in situ using the ruby R1 fluorescence line shift. The pressure value can be calculated by the equation[2,3],

$$P = \frac{1094}{B} \times \left[\left(\frac{\lambda}{\lambda_0} \right)^B - 1 \right]$$

where P is the pressure in GPa, λ_0 the wavelength of ruby R1 line in Å at zero pressure, λ the wavelength of the ruby R1 line in Å at certain pressure, and B is a constant of 7.665. Figure S2b exhibits the shift of the ruby R1 line as increasing

pressure from 0 to 4.9 GPa.

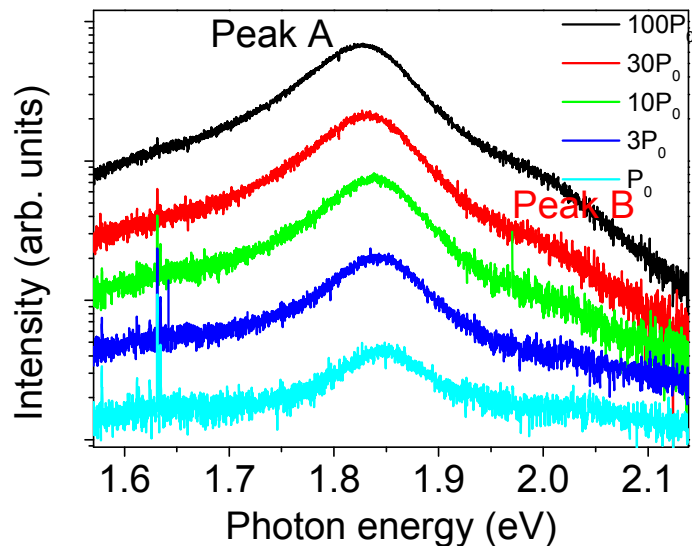**Excitation power dependence of the PL of monolayer MoS_2**

Figure S3. PL spectra of monolayer MoS_2 with increasing excitation power from P_0 to $100P_0$ with a 454 nm laser.

As can be seen in Figure S3, peak A in the PL spectra of monolayer MoS_2 exhibits a redshift of approximately 23 meV from 1.849 to 1.826 eV with increasing excitation power from P_0 to 100 P_0. At the excitation power of 100 P_0, peak B is observed at approximately 1.990 meV. As decreasing excitation power, it becomes difficult to be resolved. The redshift of the exciton A may be related to the presence of the many-body effects[4].

Interference effect in the reflectance spectra

For monolayer and few-layer MoS_2, the interference effect is observed in the reflectance spectra when the sample is put into the DAC device. The interference effect is generated between the culet face of the top diamond anvil and the surface of the sample. The effect is strengthened as increasing pressure, as shown in Figures 2a, b, and c in the main text, due to the decreasing of the distance between the culet face of the diamond anvil and the surface of the sample. In order to decreasing the interference effect, the thicker gasket with a thickness of 500 μm is used to increase the distance between them.

Band structures of monolayer, bilayer and trilayer MoS_2 at 0 and 5 GPa
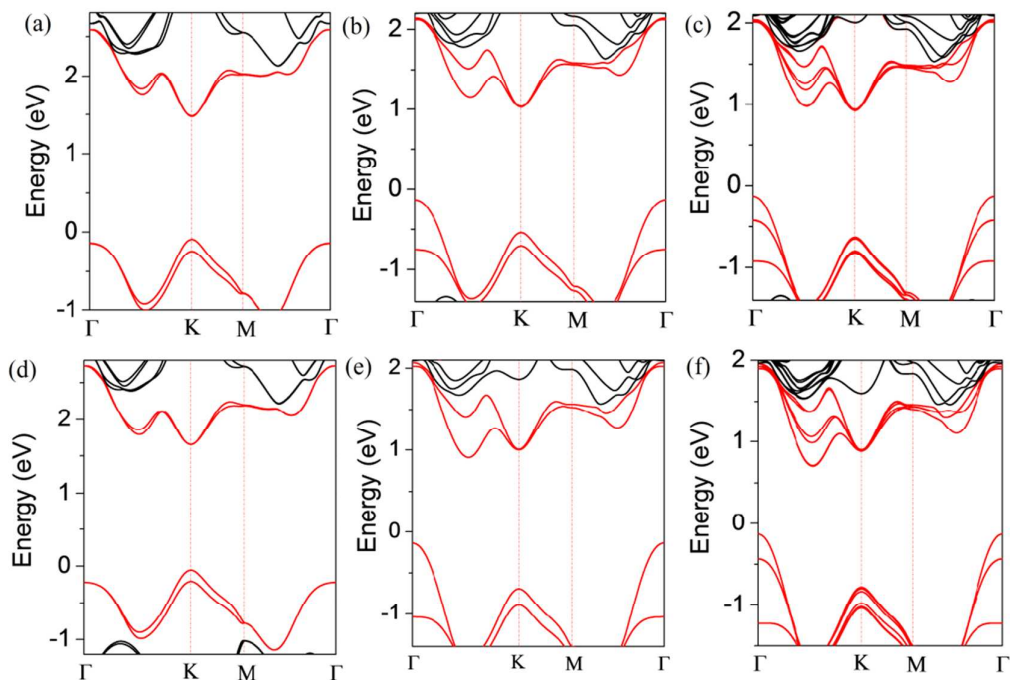
Figure S4. Band structures of monolayer (a, d), bilayer (b, e), and trilayer MoS_2 (c, f) at 0 and 5 GPa, respectively, calculated with spin-orbit coupling.

The calculated energies of excitons A, B, and C versus pressure in monolayer, bilayer and trilayer MoS_2
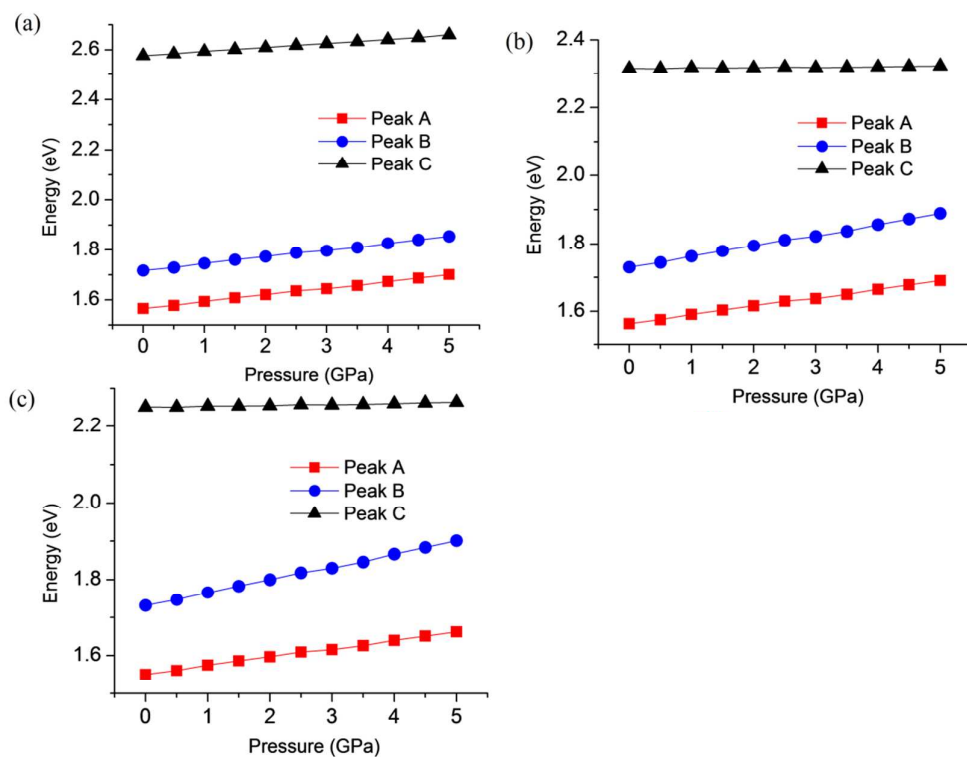
Figure S5. Energies of excitons A, B, and C as a function of pressure in monolayer (a), bilayer (b) and trilayer (c) MoS_2 calculated with spin-orbit coupling.

The calculated changes of the energies of excitons A, B, and C with increasing pressure up to 5 GPa for monolayer, bilayer and trilayer MoS_2 are shown in Figure S5 (band structures at 0 and 5 GPa shown in Figure S4). Based on the calculations, pressure coefficients (dE/dP) of peaks A, B, and C are 22.1, 22.6, and 16.8 meV/GPa in monolayer; 22.3, 31.8, and 1.5 meV/GPa in bilayer; 22.5, 33.9, and 2.5 meV/GPa in trilayer. The results are reasonable consistent with the experimental results shown in Figure 2 in the main text.

References
(1) Jayaraman, A. Diamond Anvil Cell and High-Pressure Physical Investigations. *Rev. Mod. Phys.* **1983**, 55, 65.
(2) Piermarini, G. J.; Block, S.; Barnett, J. D.; Forman, R. A. Calibration of Pressure-Dependence of R_1 Ruby Fluorescence Line to 195 kbar. *J. Appl. Phys.* **1975**, 46, 2774.
(3) Mao, H. K.; Xu, J.; Bell, P. M. Calibration of the Ruby Pressure Gauge to 800-kbar under Quasi-Hydrostatic Conditions. *J. Geophys. Res.* **1986**, 91, 4673.
(4) Sie, E. J.; Frenzel, A. J.; Lee, Y.-H.; Kong, J.; Gedik, N. Intervalley Biexcitons and Many-Body Effects in Monolayer MoS_2. *Phys. Rev. B* **2015**, 92, 125417.